NASA/CR—2004-213073

# EUPDF-II: An Eulerian Joint Scalar Monte Carlo PDF Module

## Users' Manual

M.S. Raju
QSS Group Inc., Cleveland, Ohio

April 2004

The NASA STI Program Office . . . in Profile

Since its founding, NASA has been dedicated to the advancement of aeronautics and space science. The NASA Scientific and Technical Information (STI) Program Office plays a key part in helping NASA maintain this important role.

The NASA STI Program Office is operated by Langley Research Center, the Lead Center for NASA's scientific and technical information. The NASA STI Program Office provides access to the NASA STI Database, the largest collection of aeronautical and space science STI in the world. The Program Office is also NASA's institutional mechanism for disseminating the results of its research and development activities. These results are published by NASA in the NASA STI Report Series, which includes the following report types:

- TECHNICAL PUBLICATION. Reports of completed research or a major significant phase of research that present the results of NASA programs and include extensive data or theoretical analysis. Includes compilations of significant scientific and technical data and information deemed to be of continuing reference value. NASA's counterpart of peer-reviewed formal professional papers but has less stringent limitations on manuscript length and extent of graphic presentations.

- TECHNICAL MEMORANDUM. Scientific and technical findings that are preliminary or of specialized interest, e.g., quick release reports, working papers, and bibliographies that contain minimal annotation. Does not contain extensive analysis.

- CONTRACTOR REPORT. Scientific and technical findings by NASA-sponsored contractors and grantees.

- CONFERENCE PUBLICATION. Collected papers from scientific and technical conferences, symposia, seminars, or other meetings sponsored or cosponsored by NASA.

- SPECIAL PUBLICATION. Scientific, technical, or historical information from NASA programs, projects, and missions, often concerned with subjects having substantial public interest.

- TECHNICAL TRANSLATION. English-language translations of foreign scientific and technical material pertinent to NASA's mission.

Specialized services that complement the STI Program Office's diverse offerings include creating custom thesauri, building customized databases, organizing and publishing research results . . . even providing videos.

For more information about the NASA STI Program Office, see the following:

- Access the NASA STI Program Home Page at ***http://www.sti.nasa.gov***

- E-mail your question via the Internet to help@sti.nasa.gov

- Fax your question to the NASA Access Help Desk at 301–621–0134

- Telephone the NASA Access Help Desk at 301–621–0390

- Write to:
  NASA Access Help Desk
  NASA Center for AeroSpace Information
  7121 Standard Drive
  Hanover, MD 21076

NASA/CR—2004-213073

# EUPDF-II: An Eulerian Joint Scalar Monte Carlo PDF Module

## Users' Manual

M.S. Raju
QSS Group Inc., Cleveland, Ohio

Prepared under Contract NAS3–00145

National Aeronautics and
Space Administration

Glenn Research Center

April 2004

**Acknowledgments**

The research funding for this work was provided by NASA Glenn Research Center
with Dr. N.-S. Liu acting as the technical monitor.

This report contains preliminary
findings, subject to revision as
analysis proceeds.

Available from

NASA Center for Aerospace Information
7121 Standard Drive
Hanover, MD 21076

National Technical Information Service
5285 Port Royal Road
Springfield, VA 22100

Available electronically at http://gltrs.grc.nasa.gov

# EUPDF-11: An Eulerian Joint Scalar Monte Carlo PDF Module
## Users' Manual

M.S. Raju
QSS Group, Inc.
Cleveland, Ohio 44135

## 1 ABSTRACT

EUPDF-II provides the solution for the species and temperature fields based on an evolution equation for PDF (Probability Density Function) and it is developed mainly for application with sprays, combustion, parallel computing and unstructured grids. It is designed to be massively parallel and could easily be coupled with any existing gas-phase CFD and spray solvers. The solver accommodates the use of an unstructured mesh with mixed elements of either triangular, quadrilateral, and/or tetrahedral type. The manual provides the user with an understanding of the various models involved in the PDF formulation, its code structure and solution algorithm, and various other issues related to parallelization and its coupling with other solvers. The source code of EUPDF-II will be available with National Combustion Code (NCC) as a complete package.

## 2 NOMENCLATURE

| | |
|---|---|
| $A$ | pre-exponent coefficient in an Arrhenius reaction rate term |
| $a$ | non-unity exponent in an Arrhenius reaction rate term |
| $\underline{a}_n$ | outward area normal vector of the nth surface, $m^2$ |
| $B_k$ | Spalding transfer number |
| $b$ | non-unity exponent in an Arrhenius reaction rate term |
| $C_p$ | specific heat, J/(kg K) |
| $C_\phi$ | the constant used in Eq. (7) |
| $c_n$ | convection/diffusion coefficient of the nth face, kg/s |
| $D$ | turbulent diffusion coefficient, $m^2/s$ |
| $E_a$ | activation energy in an Arrhenius reaction rate term, J/kg-mole |
| $h$ | specific enthalpy, J/kg |
| $J_i^\alpha$ | diffusive mass flux vector, kg/ms |
| $k$ | turbulence kinetic energy, $m^2/s^2$ |
| $l_k$ | mixture latent heat of evaporation, J/kg |
| $l_{k,eff}$ | effective latent heat of evaporation, J/kg (defined in Eq. (11)) |
| $l_{kin}$ | heat of vaporization at normal boiling point, J/kg |
| $M_i$ | molecular weight of ith species, kg/kg-mole |
| $m_k$ | droplet vaporization rate, kg/s |
| $N_{av}$ | number of time steps employed in the PDF time-averaging scheme |
| $N_f$ | number of surfaces contained in a given computational cell |
| $N_m$ | total number of Monte Carlo particles per grid cell |
| $N_p$ | total number of computational cells |
| $n_k$ | number of droplets in kth group |
| $P$ | pressure, $N/m^2$ |
| $P_c$ | critical pressure, $N/m^2$ |
| $P_r$ | Prandtl number |
| $p$ | joint scalar PDF |
| $R_u$ | universal gas constant, 8314.4 J/(kg-mole K) |
| $Re$ | Reynolds number |
| $s_{mlc}$ | liquid source contribution of the gas-phase continuity equation |
| $s_{mle}$ | liquid source contribution of the gas-phase energy equation |
| $s_{mlm}$ | liquid source contribution of the gas-phase momentum equations |
| $s_{mls}$ | liquid source contribution of the gas-phase species equations |
| $s_\alpha$ | liquid source contribution for the $\alpha$-th variable |
| $T$ | temperature, K |
| $T_{nb}$ | normal boiling point, K |
| $T_c$ | critical temperature, K |

| | |
|---|---|
| $t$ | time, s |
| $u_i$ | velocity, m/s |
| $V_c$ | volume of the computational cell, $m^3$ |
| $w_\alpha$ | represents the chemical reaction rate term in Eq. (5), 1/s |
| $\dot{w}_j$ | represents the chemical reaction rate term in Eq. (3), 1/s |
| $x_i$ | Cartesian coordinate in the ith direction, m |
| $y_j$ | mass fraction of jth species |
| $\underline{x}$ | spatial vector |
| $\chi$ | mole fraction |
| $\Delta t$ | local time step used in the PDF computations, s |
| $\Delta t_f$ | local time step used in the flow solver, s |
| $\Delta V$ | computational cell volume, $m^3$ |
| $\delta$ | Dirac-delta function |
| $\epsilon$ | rate of turbulence dissipation, $m^2/s^3$ |
| $\epsilon_j$ | fractional mass evaporating rate of species at the droplet surface |
| $\epsilon_{\alpha s}$ | species mass fraction at the droplet surface |
| $\Gamma_\phi$ | turbulent diffusion coefficient, kg/ms |
| $\lambda$ | thermal conductivity, J/(ms K) |
| $\mu$ | dynamic viscosity, kg/ms |
| $\omega$ | turbulence frequency, 1/s |
| $\phi$ | represents the solution field of the joint PDF transport equation |
| $\underline{\psi}$ | independent composition space |
| $\rho$ | density, $kg/m^3$ |
| $\rho_{ln}$ | liquid density (at 1 bar, 273.15 K), $kg/m^3$ |
| $\sigma$ | dimensionality of $\underline{\psi}$-space |
| $\tau$ | stress tensor term, $kg/ms^2$ |
| $\theta$ | void fraction |

**Subscripts**

| | |
|---|---|
| $f$ | represents conditions associated with fuel |
| $g$ | global or gas-phase |
| $i$ | index for the spatial coordinate or the species component |
| $j$ | index for the species component |
| $k$ | droplet group or liquid-phase |
| $l$ | liquid-phase |
| $m$ | conditions associated with $N_m$ |
| $n$ | nth-face of the computational cell |
| $o$ | either initial conditions or oxidizer |
| $p$ | conditions associated with the properties of a grid cell |
| $s$ | represents conditions at the droplet surface or adjacent computational cell |
| $t$ | conditions associated with time |
| $\alpha$ | index for the scalar component of the joint PDF equation |
| , | partial differentiation with respect to the variable followed by it |
| $\sigma$ | the total number of composition variables in Eq. (5) |

**Superscripts**

| | |
|---|---|
| ~ | Favre averaging |
| - | time averaging or average based on the Monte Carlo particles present in a given cell |
| $\star$ | the solution step associated with Eq. (14) |
| $\star\star$ | the solution step associated with Eq. (15) |
| $\star\star\star$ | the solution step associated with Eq. (16) |
| $''$ | fluctuations |

## 3 INTRODUCTION

The gas-turbine combustor flows are often characterized by a complex interaction between various physical processes such as the interaction between the liquid and gas phases, heat release associated with chemical kinetics, and radiative heat transfer associated with highly absorbing and radiating species. The rate controlling processes often interact with each other at various disparate time and length scales. In particular, turbulence plays an important role in determining the rates of mass transfer, heat transfer, chemical reactions, and droplet evaporation. Most of the turbulence closure models for reactive flows have difficulty in treating nonlinear reaction rates [1-2]. The use of assumed shape PDF methods was found to provide reasonable predictions for pattern factors and $NO_X$ emissions at the combustor exit. However, their extension to multi-scalar chemistry becomes quite intractable. The solution procedure based on the modeled joint scalar PDF transport equation has an advantage in that it treats the nonlinear reaction rates without any approximation. In this approach, the velocity and turbulence fields are solved using a conventional CFD solver, a modeled PDF transport equation provides the solution for the species and temperature fields, and an appropriate spray formulation is used for the liquid-phase representation. The method based on the combined PDF/CFD/spray calculations holds the promise of providing an accurate representation for several important combustion phenomena associated with the prediction of emissions (CO and $NO_X$), UHC (Unburnt HydroCarbons), and flame extinction and blow-off limits [1].

However, one of the major disadvantages of this method is that all of the composition variables

also appear as the independent variables of the PDF transport equation. Because of the large dimensionality, it is almost impossible to obtain a solution for the joint scalar PDF transport equation based on conventional finite-difference techniques [1]. However, Monte Carlo methods are better suited for obtaining a solution to this PDF equation because it was shown that the required computational effort increases only linearly with the increase in the dimensionality of the PDF transport equation [1]. Other than some application to simple flows, there is a very limited evidence of the application of this method to the calculation of practical combustion flows [3]. It is because the Monte Carlo methods tend to be both computationally very time consuming and require a large computer memory for application to 3D flows [3]. However, the success of any numerical tools used in multidimensional combustor modeling depends not only on the modeling- and numerical-accuracy requirements but also on the computational-efficiency considerations as determined by the computer memory and turnaround times afforded by the present-day computers. With the aim of demonstrating its viability to flows representative of a gas-turbine combustor, we have undertaken the task of extending this technique in a number of significant ways:

1. In order to demonstrate the importance of chemistry/turbulence interactions in the modeling of reacting sprays, we have extended the joint scalar Monte Carlo PDF approach to the modeling of spray flames.

2. It facilitates the use of both unstructured grids and parallel computing and, thereby, facilitating large-scale combustor computations involving complex geometrical configurations.

3. We have developed and implemented several numerical convergence techniques such as local time-stepping and various other averaging methods in order to accelerate convergence to a steady state.

4. The PDF method provided favorable agreement when applied to several supersonic diffusion flames as well as several other subsonic spray flames [4-9].

Some of our work on the Monte Carlo PDF method could be found in Refs. [4-9]. Initially, the emphasis of our work was on extending this technique to the modeling of compressible reacting flows [4]. The Monte Carlo solver was used in conjunction with several density-based CFD codes for the mean-velocity and turbulence fields. Several averaging procedures introduced in Refs. [4-5] proved to be useful in providing smooth Monte Carlo solutions to the CFD solver. The PDF method provided favorable results when applied to several supersonic diffusion flames [4-5].

Later on this approach was further extended to the modeling of spray flames and parallel computing and, thereby, combining the novelty of the PDF method with the ability to run on parallel architectures [6]. This algorithm was implemented on the Cray T3D at NASA Lewis Research Center, a massively parallel computer, with an aggregate of 64 Processor Elements (PEs). The computer code was written in Cray MPP (Massively Parallel Processing) Fortran. The application of this method to both open as well as confined axisymmetric swirl-stabilized spray flames showed reasonable agreement with the measured data [6].

With the aim of advancing the current multidimensional computational tools used in the design of advanced technology combustors, two new computer codes, LSPRAY - a Lagrangian spray solver [10] and EUPDF - an Eulerian Monte Carlo PDF solver [11], were developed, thereby extending our previous work [6] on the Monte Carlo PDF and sprays to unstructured grids as a part of NCC development. The combined unstructured 3D CFD/Spray/Monte-Carlo-PDF solver is designed to be massively parallel and accommodates the use of an unstructured mesh with mixed elements comprised of either triangular, quadrilateral, and/or tetrahedral type. This was done mainly to facilitate representation of complex geometries with relative ease [7-9]. Also, it is noteworthy that considerable effort usually goes into the grid generation of practical combustion devices which tend to be very complex in both shape and configuration. The grid generation time could be reduced considerably by making use of existing unstructured grid generators such as GRIDGEN. A current status of the use of the parallel computing in turbulent reacting flows involving sprays, scalar Monte Carlo PDF and unstructured grids was described in Ref. [7]. It outlined several numerical techniques developed for overcoming some of the high computer time-and-storage requirements associated with the use of Monte Carlo solution methods. The parallel performance of both the PDF and CFD computations was found to be excellent but the results on the

spray computations showed reasonable performance. Our preliminary estimates indicated that it was well within the reach of modern parallel computer's capacity to perform a realistic gas-turbine combustor simulation [6-9].

Some salient features of the Monte Carlo PDF module are summarized below:

1. The scalar Monte Carlo PDF solver has been extended to mixed unstructured grid elements of triangular, quadrilateral, tetrahedron, wedge, and hexahedron elements.

2. EUPDF-II is currently coupled with an unstructured flow (CFD) solver of NCC [12-13], and a Lagrangian spray solver - LSPRAY [10], which were selected to be as the integral components of the NCC cluster of modules.

3. The PDF code receives the mean velocity and turbulence fields from the flow solver. And, also, it receives the source terms arising from the liquid-phase contribution from the spray solver if needed.

4. The PDF solver provides the species and temperature solution to the CFD solver and, also, to the spray solver if needed.

5. The PDF code is written in Fortran 77/90 with PVM or MPI calls for parallel computing. It enables the computations to be performed with equal ease on both massively parallel computers as well as workstation clusters.

The furnished code demonstrates the successful methods used for parallelization and coupling of the PDF to the flow code. First, complete details of the Monte Carlo PDF solution procedure is presented along with several other numerical issues related to the coupling between the CFD, EUPDF-II, and LSPRAY modules. It is followed by a brief description of the combined parallel performance of the three solvers (CFD, EUPDF-II, and LSPRAY) along with a brief summary of the validation cases.

## 4 GOVERNING EQUATIONS FOR THE GAS PHASE

Here, we summarize the conservation equations for the gas-phase in Eulerian coordinates [14]. These equations are valid for a dilute spray with a void fraction of the gas, $\theta$, close to unity. The void fraction is defined as the ratio of the equivalent volume of gas to a given volume of a gas and liquid mixture. This is done for the purpose of identifying the interphase source terms arising from the exchanges of mass, momentum, and energy with the liquid-phase.

The conservation of the mass leads to:

$$[\bar{\rho}V_c]_{,t} + [\bar{\rho}V_c u_i]_{,x_i} = s_{mlc} = \sum_k n_k \, m_k \qquad (1)$$

For mass conservation, the source term is given as a summation over different classes of droplets. Each class represents the average properties of a different polydisperse group of droplets. Here, $n_k$ represents the number of droplets in a given class and $m_k$ represents the corresponding mass vaporization rate.

For the conservation of the jth species, we have:

$$[\bar{\rho}V_c y_j]_{,t} + [\bar{\rho}V_c u_i y_j]_{,x_i} - [\bar{\rho}V_c D y_{j,x_i}]_{,x_i}$$
$$-\bar{\rho}V_c \dot{w}_j = s_{mls} = \sum_k \epsilon_j \, n_k \, m_k \qquad (2)$$

where

$$\sum_j \dot{w}_j = 0 \; and \; \sum_j \epsilon_j = 1$$

For the species conservation, the source term contains an additional variable, $\epsilon_j$, which is defined as the fractional vaporization rate for species $j$.

For the momentum conservation, we have:

$$[\bar{\rho}V_c u_i]_{,t} + [\bar{\rho}V_c u_i u_j]_{,x_j} + [pV_c]_{,x_i} -.$$
$$[\theta V_c \tau_{ij}]_{,x_j} - [(1-\theta)V_c \tau_{lij}]_{,x_j} = s_{mlm} =$$
$$\sum_k n_k \, m_k \, u_{ki} - \sum_k \frac{4\pi}{3} \rho_k \, r_k^3 \, n_k \, u_{ki,t} \qquad (3)$$

where the shear stress $\tau_{ij}$ in Eq. (3) is given by:

$$\tau_{ij} = \mu[u_{i,x_j} + u_{j,x_i}] - \frac{2}{3}\mu\delta_{ij}u_{i,x_j}$$

For the momentum conservation, the first source term represents the momentum associated with liquid fuel vapor and the second represents the momentum change associated with droplet drag.

For the energy conservation, we have:

$$[\bar{\rho}V_c h]_{,t}+[\bar{\rho}V_c u_i h]_{,x_i}-[\theta V_c \lambda T_{,x_i}]_{,x_i}-[(1-\theta)V_c\lambda_l T_{,x_i}]_{,x_i}$$
$$-[\theta V_c p]_{,t} = s_{mle} = \sum_k n_k\, m_k\Big(h_s - l_{k,eff}\Big) \quad (4)$$

Similarly, the energy conservation has a source first term associated with liquid fuel vapor and the second represents the heat loss associated with the latent heat of vaporization and it also contains an additional heat flux (loss or gain) to the droplet interior from the ambient.

The main purpose of the spray solver is to calculate the source terms arising from the exchanges of the mass, momentum, and energy and, then, feed that appropriate information to the gas-phase solver. In the case of NCC, it supplies the source terms to the CFD solver and, also, to the Monte Carlo PDF solver if needed.

## 5 GAS-PHASE SCALAR JOINT PDF EQUATION

The transport equation for the density-weighted joint PDF of the compositions, $\tilde{p}$, is:

$$\underbrace{\bar{\rho}[\tilde{p}]_{,t}}_{\{Transient\}} + \underbrace{\bar{\rho}\tilde{u}_i[\tilde{p}]_{,x_i}}_{\{Mean\ convection\}}$$
$$+\underbrace{[\bar{\rho}w_\alpha(\underline{\psi})\tilde{p}]_{,\psi_\alpha}}_{\{Chemical\ reactions\}} = \underbrace{-[\bar{\rho}<u_i''\mid\underline{\psi}>\tilde{p}]_{,x_i}}_{\{Turbulent\ convection\}}$$
$$\underbrace{-[\bar{\rho}<\frac{1}{\rho}J^\alpha_{i,x_i}\mid\underline{\psi}>\tilde{p}]_{,\psi_\alpha}}_{\{Molecular\ mixing\}} \underbrace{-[\bar{\rho}<\frac{1}{\rho}s_\alpha\mid\underline{\psi}>\tilde{p}]_{,\psi_\alpha}}_{\{Liquid-phase\ contribution\}} \quad (5)$$

where

| | | |
|---|---|---|
| $w_\alpha$ | = | chemical source term for the $\alpha$-th composition variable, |
| $<u_i''\mid\underline{\psi}>$ | = | conditional average of Favre velocity fluctuations, |
| $<\frac{1}{\rho}J^\alpha_{i,x_i}\mid\underline{\psi}>$ | = | conditional average of scalar dissipation, & |
| $<\frac{1}{\rho}s_\alpha\mid\underline{\psi}>$ | = | conditional average of spray source terms. |

The terms on the left-hand side of the above equation could be evaluated without any approximation, but the terms on the right-hand side of the equation require modeling. The first term on the right represents transport in physical space due to turbulent convection [1]. Since the joint PDF, $\tilde{p}$, contains no information on velocity, the conditional expectation of $<u_i''\mid\underline{\psi}>$ needs to be modeled. It is modeled based on a gradient-diffusion model with information supplied on the turbulent flow field from the flow solver [1].

$$-<u_i''\mid\underline{\psi}>\tilde{p} = \Gamma_\phi\tilde{p}_{,x_i} \quad (6)$$

The fact that the turbulent convection is modeled as a gradient-diffusion makes the turbulent model no better than the $k-\epsilon$ model. However, it is noteworthy that the option of using a non-linear $k-\epsilon$ turbulence model of Shih et al. [15], seems to alleviate some of the modeling uncertainties associated with the use of the standard $k-\epsilon$ model.

The second term on the right-hand side represents transport in the scalar space due to molecular mixing. A mathematical description of the mixing process is rather complicated, and the interested reader is referred to Ref. 2. Molecular mixing is accounted for by making use of the relaxation to the ensemble mean submodel [2].

$$<\frac{1}{\rho}J^\alpha_{i,x_i}\mid\underline{\psi}>= -C_\phi\omega(\phi_\alpha-\bar{\phi}_\alpha) \quad (7)$$

where $\omega = \epsilon/k$, and $C_\phi$ is a constant. For a conserved scalar in a homogeneous turbulence, this model preserves the PDF shape during its decay, but there is no relaxation to a Gaussian distribution [1]. However, the results of Ref. 16 indicate that the choice between different widely-used mixing models is not critical in the distributed reaction regime of premixed combustion as long as the turbulent mixing frequencies are above 1000 Hz. Most practical combustors seem to operate at in-flame mixing frequencies of 1000 Hz and above. The application of this mixing model seemed to provide some satisfactory results when applied to flows representative of those encountered in the gas-turbine combustion [16].

The third term on the right-hand side represents the contribution from the spray source terms:

$$<\frac{1}{\rho}s_\alpha\mid\underline{\psi}>= \frac{1}{\bar{\rho}\Delta V}\sum n_k m_k(\epsilon_{\alpha s}-\phi_\alpha) \quad (8)$$

where $\phi_\alpha = y_\alpha \ \ when\ \alpha = 1,2,...,\sigma-1$

$$<\frac{1}{\rho}s_\alpha\mid\underline{\psi}>= \frac{1}{\bar{\rho}\Delta V}\sum n_k m_k(-l_{k,eff}+h_{ks}-\phi_\alpha) \quad (9)$$

where $\phi_{\alpha=\sigma} = h$ and is defined by:

$$h = \sum_{i=1}^{\sigma-1} y_i h_i \tag{10}$$

where

$$h_i = h_{fi}^o + \int_{T_{ref}}^{T} C_{pi} y_i dT,$$

$$C_{pi} = \frac{R_u}{W_i}(A_{1i} + A_{2i}T + A_{3i}T^2 + A_{4i}T^3 + A_{5i}T^4),$$

$h_{fi}^o$ is the heat of formation of ith species, $R_u$ is the universal gas constant, $\epsilon_{\alpha s}$ is the fractional mass evaporating rate of species at the droplet surface, and $l_{k,eff}$ is the effective latent heat of vaporization as modified by the heat loss to the droplet interior:

$$l_{k,eff} = l_k + 4\pi \frac{\lambda_l r_k^2}{m_k} \left(\frac{\partial T_k}{\partial r}\right)_s \tag{11}$$

where the mixture latent heat of vaporization, $l_k$, is given by

$$l_k = \sum_i \delta_i l_{ki},$$

$$l_{ki} = l_{kin}\left(\frac{T_{ci} - T}{T_{ci} - T_{bi}}\right)^{0.38},$$

and

$$T_{bi} = \frac{l_{kin} M_i / R_u}{l_{kin} M_i / (R_u t_{bni}) - ln(p)}$$

More details on Eq. (11) can be found in a companion report on LSPRAY-II: a Lagrangian spray module.

## 6 PDF SOLUTION ALGORITHM

Partial finite-differencing and rearrangement of the terms associated with the convection and diffusion of Eq. (5) yields:

$$\tilde{p}_p(\underline{\psi}, t + \Delta t) = (1 - \frac{c_p \Delta t}{\bar{\rho} \Delta V})\tilde{p}_p(\underline{\psi}, t)$$

$$+ \sum_n \frac{c_n \Delta t}{\bar{\rho} \Delta V} \tilde{p}_n(\underline{\psi}, t) - \Delta t[w_\alpha(\underline{\psi})\tilde{p}]_{,\psi_\alpha}$$

$$-\Delta t[< \frac{1}{\rho} J_{i,x_i}^{\alpha} \mid \underline{\psi} > \tilde{p}]_{,\psi_\alpha} - \Delta t[< \frac{1}{\rho} s_\alpha \mid \underline{\psi} > \tilde{p}]_{,\psi_\alpha} \tag{12}$$

where the subscript $n$ refers to the nth-face of the computational cell. The coefficient $c_n$ represents the combined flux in physical space due to convection and diffusion through the nth-face of the computational cell, $p$. The convection/diffusion coefficients in the above equation are determined by one of the following two expressions:

$$c_n = \Gamma_\phi(\frac{2\underline{a}_n \cdot \underline{a}_n}{\Delta V_p + \Delta V_s}) + max[0, -\bar{\rho}\underline{a}_n \cdot \underline{u}_n]$$

$$c_n = max[|0.5\bar{\rho}\underline{a}_n \cdot \underline{u}_n|, \Gamma_\phi(\frac{2\underline{a}_n \cdot \underline{a}_n}{\Delta V_p + \Delta V_s})\,] - 0.5\bar{\rho}\underline{a}_n \cdot \underline{u}_n$$

and

$$c_p = \sum_n c_n$$

In both the above expressions for $c_n$, a cell-centered finite-volume derivative is used to describe the viscous fluxes; but an upwind differencing scheme is used for the convective fluxes in the first expression and a hybrid differencing scheme in the second.

### 6.1 Numerical Method Based on Approximate Factorization

The transport equation is solved by making use of an approximate factorization scheme [1]. Eq. (12) can be recast as:

$$\tilde{p}_p(\underline{\psi}, t + \Delta t) =$$

$$(I + \Delta t R)(I + \Delta t S)(I + \Delta t M)(I + \Delta t T)\tilde{p}_p(\underline{\psi}, t) + O(\Delta t^2) \tag{13}$$

where $I$ represents the unity operator and $T$, $M$, $S$, and $R$ denote the operators associated with spatial transport, molecular mixing, spray, and chemical reactions, respectively. The operator is further split into a sequence of intermediate steps:

$$\tilde{p}_p^{\star}(\underline{\psi}, t) = (I + \Delta t T)\tilde{p}_p(\underline{\psi}, t) \tag{14}$$

$$\tilde{p}_p^{\star\star}(\underline{\psi}, t) = (I + \Delta t M)\tilde{p}_p^{\star}(\underline{\psi}, t) \tag{15}$$

$$\tilde{p}_p^{\star\star\star}(\underline{\psi}, t) = (I + \Delta t S)\tilde{p}_p^{\star\star}(\underline{\psi}, t) \tag{16}$$

$$\tilde{p}_p(\underline{\psi}, t + \Delta t) = (I + \Delta t R)\tilde{p}_p^{\star\star\star}(\underline{\psi}, t) \qquad (17)$$

The operator-splitting method is used to provide the solution for $\tilde{p}$ by making use of a Monte Carlo technique. In the Monte Carlo simulation, the continuos PDF is replaced by a a discrete PDF which is defined in terms of a large ensemble of stochastic particles. The ensemble-averaged PDF over $N_m$ delta functions replaces the average based on a continuous PDF [1].

$$\tilde{p}_{pm}(\psi) = < \tilde{p}_p(\psi) > = \frac{1}{N_m} \sum_{n=1}^{N_m} \delta(\psi - \phi^n) \qquad (18)$$

The discrete PDF $\tilde{p}_{pm}(\psi)$ is defined in terms of an ensemble of $N_m$ Dirac-delta functions each associated with a corresponding set of $\phi^n$, $n = 1, 2, 3...N_m$. The statistical error in this approximation is proportional to $N_m^{-1/2}$.

Using the operator-splitting method, the steps associated with the spatial transport due to convection and turbulent diffusion as well as the steps associated with the transport in the scalar space due to molecular mixing, spray contribution, and chemical kinetics are advanced in a series of sequential steps as given by Eqs. (14)-(17).

### 6.2 Convection/Diffusion Step

The first step associated with convection/diffusion is given by:

$$\tilde{p}_p^{\star}(\underline{\psi}, t) = (I + \Delta t T)\tilde{p}_p(\underline{\psi}, t) =$$
$$(1 - \frac{c_p \Delta t}{\bar{\rho}\Delta V})\tilde{p}_p(\underline{\psi}, t) + \sum_n \frac{c_n \Delta t}{\bar{\rho}\Delta V}\tilde{p}_n(\underline{\psi}, t) \qquad (19)$$

This step is simulated by replacing a randomly selected number of particles as given by $\phi_p^1(t)$,..,$\phi_p^{N_t}(t)$ ($N_t$ = the nearest integer of $\frac{c_n \Delta t N_m}{\bar{\rho}\Delta V}$) with by a set of the same number of randomly selected particles chosen from the neighboring cell located on the opposite side of the corresponding n-th face.

### 6.3 Numerical Issues Associated With Fixed Versus Variable Time Step

It is obvious from the above equation that a necessary criterion for stability requires satisfaction of $\frac{c_p \Delta t}{\bar{\rho}\Delta V} < 1$. When the computations are performed with a fixed time step, this criterion tends to be too restrictive for most applications. Depending on the flow configuration, the allowable maximum time increment $\Delta t$ is likely to be limited by a region of the flow field where convective fluxes dominate (such as close to injection holes). But in the main stream, the flow is usually characterized by much lower velocities. Resolution considerations require a higher concentration of the grid in certain regions of the flow-field than in others. For example, more grid cells are clustered in regions where boundary layers are formed. In such regions the allowable maximum time increment might be limited in a direction dominated by the largest of the diffusive fluxes as determined by $\Gamma_\phi/\Delta x$. This problem gets magnified if the cells also happen to be highly skewed.

Such restrictions on the allowable maximum time step could lead to a frozen condition when the Monte Carlo simulation is performed with a limited number of stochastic particles per cell. For clarity, let us consider the following criterion:

$$N_m > \frac{\bar{\rho}\Delta V}{c_n \Delta t} \qquad (20)$$

which has to be satisfied at all grid nodes. It is estimated that about $10^3$ stochastic particles per cell are needed in order to avoid the so-called frozen condition for performing a typical 3-D gas-turbine combustor calculation. The frozen condition is referred to as a state in which no transfer of stochastic particles takes place between the neighboring cells when $N_m$ falls below a minimum required. Scheurlen et al. [3] were the first ones to recognize the limitations associated with the use of a fixed time step in the Monte Carlo PDF computations.

However, our experience has shown that this problem can be overcome by introducing the concept of local time-stepping which is a convergence improvement technique widely used in many of the steady-state CFD computations. In this approach, the solution is advanced by making use of a local time step which could be different at each one of its computational nodes. In our present computations, it is determined based on

$$\Delta t = min(C_{tf}\Delta t_f, \frac{\rho \Delta V}{C_t c_n}) \qquad (21)$$

where $C_{tf}$ and $C_t$ are calibrated constants, $\Delta t_f$ is the local time step obtained from the flow module. The local time step is chosen such that it permits transfer of enough particles across the boundaries of the

neighboring cells while ensuring that the time step used in the PDF computations does not deviate considerably from the time step used in the CFD solver.

### 6.4 Molecular Mixing Step

The second step associated with molecular mixing is given by:

$$\frac{d\phi_\alpha}{dt} = -C_\phi \omega(\phi_\alpha - \bar{\phi}_\alpha) \quad (22)$$

where $C_\phi$ is an empirical constant with a value of about unity.

The solution for this equation is updated by:

$$\phi_\alpha^{\star\star} = \phi_\alpha^{\star} + (\phi_\alpha^{\star} - \bar{\phi}_\alpha^{\star})e^{-C_\phi \omega \Delta t} \quad (23)$$

### 6.5 Spray Step

The third step associated with the spray contribution is given by:

$$\frac{d\phi_\alpha}{dt} = \frac{1}{\bar{\rho}\Delta V}\sum n_k m_k(\epsilon_\alpha - \phi_\alpha) \quad (24)$$

where $\phi_\alpha = y_\alpha \; when \; \alpha = 1, 2, ..., \sigma - 1$

$$\frac{d\phi_\alpha}{dt} = \frac{1}{\bar{\rho}\Delta V}\sum n_k m_k(-l_{k,eff} + h_{ks} - \phi_\alpha) \quad (25)$$

where $\phi_\alpha = h$ when $\alpha = \sigma$ The solution for the above equations is upgraded by a simple explicit scheme:

$$\phi_\alpha^{\star\star\star} = \epsilon_\alpha \frac{\Delta t \sum n_k m_k}{\bar{\rho}\Delta V} + \phi_\alpha^{\star\star}(1 - \frac{\Delta t \sum n_k m_k}{\bar{\rho}\Delta V}) \quad (26)$$

where $\alpha \leq \sigma - 1$

$$\phi_\alpha^{\star\star\star} = \frac{\Delta t \sum n_k m_k}{\bar{\rho}\Delta V}(-l_{k,eff} + h_{ks}) + \phi_\alpha^{\star\star}(1 - \frac{\Delta t \sum n_k m_k}{\bar{\rho}\Delta V}) \quad (27)$$

where $\alpha = \sigma$. After a new value for enthalpy is updated, the temperature is determined iteratively from the solution of Eq. (10).

### 6.6 Reaction Step

Finally, the fourth step associated with chemical reactions is given by:

$$\frac{d\phi_\alpha}{dt} = -\nu_f \frac{W_f}{\rho} A(\frac{\rho\phi_f}{W_f})^a(\frac{\rho\phi_o}{W_o})^b e^{-(\frac{E_a}{R_u T})} \quad (28)$$

where $\phi_\alpha = y_f$.

$$\frac{d\phi_\alpha}{dt} = -\nu_o \frac{W_o}{\rho} A(\frac{\rho\phi_f}{W_f})^a(\frac{\rho\phi_o}{W_o})^b e^{-(\frac{E_a}{R_u T})} \quad (29)$$

where $\phi_\alpha = y_o$.

$$\frac{d\rho\phi_\alpha}{dt} = 0 \quad (30)$$

where $\phi_\alpha = h$.

The numerical solution for Eqs. (28)-(30) is obtained by an implicit Euler scheme [17]. The resulting non-linear algebraic equations are solved by the method of quasi-linearization [18].

### 6.7 Details of Combustion Chemistry

In this section, we present an example of how combustion chemistry is handled for the case of n-heptane when it is modeled by a single-step global mechanism of Westbrook and Dryer [19]. The corresponding rate constants in Eqs. (28)-(29) are given by $A = 0.286E + 10$, $a = 0.25$, $b = 1.25$, and $E_a = 0.151E + 05$. This global combustion mechanism was reported to provide adequate representation for temperature histories in flows not dominated by long ignition delay times. For example, the overall reaction representing the oxidation involving n-heptane is given by:

$$C_7H_{16} + 11(O_2 + 3.76N_2) \rightarrow 7CO_2 + 8H_2O + 41.36N_2 \quad (31)$$

Because of the constant-Schmidt-number assumption made in the PDF formulation and based on atomic balance of the constituent species, the mass fractions of $N_2$, $CO_2$, and $H_2O$ can be shown to be related to the mass fractions of $O_2$ and $C_7H_{16}$ by the following expressions:

$$y_{H_2O} = K_2 - K_1K_2y_{O_2} - K_2y_{C_7H_{16}}$$

$$y_{CO_2} = K_3y_{H_2O} \quad (32)$$

$$y_{N_2} = 1 - K_2 - K_2K_3 - y_{O_2}(1 - K_1K_2 - K_1K_2K_3) -$$

$$y_{C_7H_{16}}(1 - K_2 - K_2K_3)$$

where $K_1 = 4.29$, $K_2 = 0.08943$, and $K_3 = 2.138$.

Making use of Eq. (32) leads to a considerable savings in computational time as it reduces the number of variables in the PDF equation from five (four species and one energy) to three (two species and one energy).

### 6.8 Revolving Time-Weighted Averaging

It is noteworthy that although local time-stepping seems to overcome some of the problems associated with the PDF computations, the application of the Monte Carlo method requires the use of a large number of particles, because the statistical error associated with the Monte Carlo Method is proportional to the inverse square root of $N_m$, thereby, making the use of the Monte Carlo method computationally very time consuming. However, a revolving averaging procedure used in Ref. 4 seems to alleviate the need for using a large number of stochastic particles, $N_m$, needed in any given single time step. In this averaging scheme, the solution provided to the CFD solver is based on an average of all the particles present over the last $N_{av}$ time steps instead of an average solely based on the number of particles present in any one single time step. This approach seemed to provide smooth Monte Carlo solutions to the CFD solver, thereby improving the convergence of the coupled CFD and Monte Carlo computations. The reason for improvement could be attributed to an effective increase in the number of stochastic particles from $N_m$ to $N_{av}N_m$. Here, the solution contained within different iterations of the averaging procedure is assumed to be statistically independent of each other.

## 7 DETAILS OF THE COUPLING BETWEEN EUPDF-II AND THE OTHER SOLVERS

- The PDF code is designed to be a stand-alone computer code which could easily be coupled with any of the other unstructured-grid CFD solvers (However, some grid-related parameters on area vectors, grid connectivity, etc. need to be supplied separately).

- The PDF solver needs information on the mean gas velocity, turbulent diffusivity and frequency from the CFD solver and the liquid-phase source terms from the spray solver.

- The PDF solver provides the solution for the species and energy fields to the CFD and spray solvers.

- It should also be noted that the PDF solver is called once at every other specified number of CFD iterations.

- All of the three solvers (LSPRAY, EUPDF-II, and CFD) are advanced sequentially in an iterative manner until a converged solution is obtained.

- All three modules (LSPRAY, EUPDF-II, and CFD) were coupled and parallelized in such a way to achieve maximum efficiency.

The coupling issues could be better understood through the use of a flow chart shown in Fig. 1. It shows the overall flow structure of the combined CFD, EUPDF-II, and LSPRAY modules. Both the PDF and spray codes are loosely coupled with the CFD code. The PDF code is designed in such a way that only a minimal a minimal amount of effort is needed for its coupling with the flow and spray solvers. The present version of the CFD module relies entirely on the use of Fortran common blocks for its information exchange with other modules. Even this reliance should entail only few changes to be made within the PDF code for its linkage with different solvers. The spray code is also structured along similar coupling principles.

The flow chart of Fig. 1 contains several blocks - some shown in black and/or solid lines and the others in color and/or dashed lines. The ones in solid blocks represent the flow chart that is typical of a CFD solver. The ones in dashed blocks represent the additions arising from the coupling of the PDF and spray modules.

The coupling starts with the calling of the subroutine - **spray_pdf_read_parameters**, which then reads the PDF control parameters from the input file, *ncc_pdf.in* of Table 1. The table provides a detailed description of the following input variables - ipdf_mod, ipdf_num, nparti, cmmx, schmit_number, ave_weight, nrollr, pdf_cfl, pdf_vardt_fac, pdf_max_dt, iran_seed.

The coupling is then followed by the calling of the **pdf_int_rerun** subroutine. It initializes PDF computations and, also, it may restart the PDF computations if needed from the data stored from a previous iteration. Similarly, we call **spray_int_rerun**

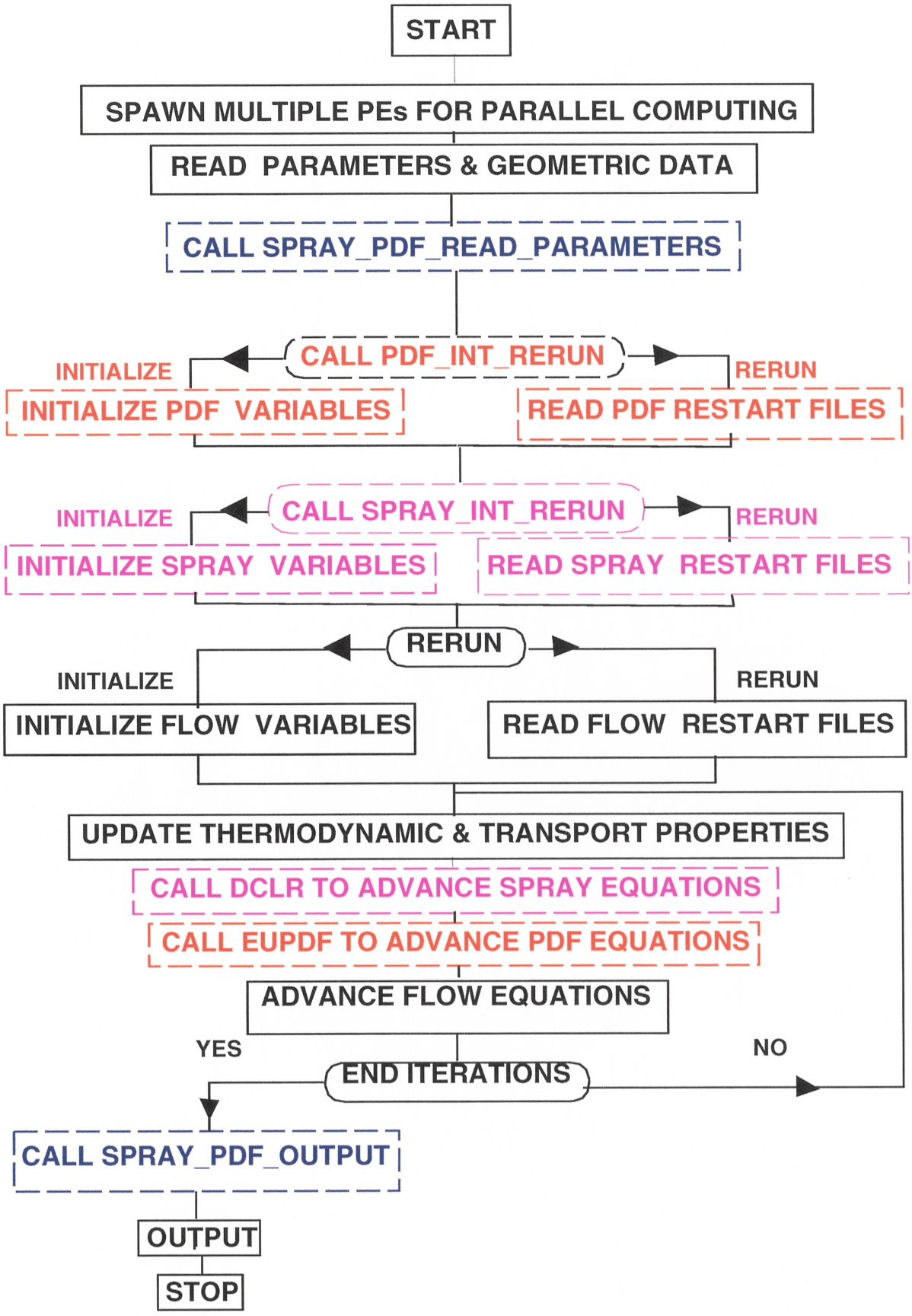


Fig. 1 The overall flow structure of the combined CFD, LSPRAY, and EUPDF–II solvers.

Table 1. ncc_pdf.in file.

| **Input file content** | **comments** |
|---|---|
| heading | title of controlling parameters |
| ipdf_mod,ipdf_num | The variable, ipdf_mod, controls the calls to the Monte Carlo PDF solver, **eupdf**. The PDF solver is called once at every other number of CFD iterations as specified by ipdf_mod.<br><br>When **eupdf** is called, it integrates the PDF computations over a fixed number of iterations as given by the number, ipdf_num. |
| heading | title of controlling parameters |
| nparti, cmmx, schmit_number, ave_weight, nrollr | nparti = $N_m$, and it represents is the number of Monte Carlo Particles per grid cell.<br><br>cmmx = $c_\phi$, and it represents the constant used in the molecular mixing model.<br><br>schmit_number is used in the calculation of $\Gamma_\phi$ of the convection/diffusion step.<br><br>ave_weight has two functions: (1) A positive value for it invokes the first averaging scheme and its actual value represents the averaging averaging weight (For details, refer to Ref. 5). (2) A negative value for it invokes the second averaging scheme described in Section 6.8.<br><br>nrollr = $N_{av}$, and it represents the number of PDF time steps employed in the PDF time-averaging scheme of Section 6.8. |
| heading | title of controlling parameters |
| pdf_cfl, pdf_vardt_fac, pdf_max_dt, iran_seed | pdf_cfl represents the constant, $C_{tf}$ used in Eq. (21).<br><br>pdf_vardt_fac represents the constant, $C_t$ used in Eq. (21).<br><br>pdf_max_dt is the maximum time step permitted in the PDF computations.<br><br>iran_seed is the seed number for use in the random number generation. |

for the spray computations. It is noteworthy that the PDF computations can be restarted by reading the data from the restart files - *ncc_pdf_params.out*, *ncc_pdf_results.db*, & *ncc_pdf_results_ave.db*. This restart capability is invoked automatically if the needed restart files exist in the run-time working directory. Otherwise, the PDF computations are initialized to start from the beginning. Then, the coupling proceeds with the calling of the following subroutines: **dclr** for integrating the spray calculations and **eupdf** for the Monte Carlo PDF. The input variable, ipdf_mod of Table 1, controls the calls to the PDF integration routine, **eupdf**. The PDF solver is called once at every other number of CFD iterations as specified by ipdf_mod. And every time the subroutine, **eupdf**, is called it integrates the pdf computations over a fixed number of iterations as given by the input variable, ipdf_num, of Table 1. Finally, the coupling ends with the calling of a subroutine, **spray_pdf_output**, which will create a set of new restart files.

## 8 DETAILS OF THE FORTRAN SUBROUTINES

Table 2 provides a list of all the Fortran subroutines developed as a part of the Monte Carlo PDF module. It also describes the purpose of all the individual subroutines.

## 9 PARALLELIZATION

There are several issues associated with the parallelization of both the spray & PDF computations. The goal of the parallel implementation is to extract maximum parallelism so as to minimize the execution time for a given application on a specified number of processors [20]. Several types of overhead costs are associated with parallel implementation which include data dependency, communication, load imbalance, arithmetic, and memory overheads. The term arithmetic overhead is the extra arithmetic operations required by the parallel implementation. Memory overhead refers to the extra memory needed. Excessive memory overhead reduces the size of a problem that can be run on a given system and the other overheads result in performance degradation [20]. Any given application usually consists of several different phases that must be performed in certain sequential order. The degree of parallelism and data dependencies associated with each of the subtasks can vary widely [20]. The goal is to achieve maximum efficiency with a reasonable programming effort [20].

In our earlier work, we discussed the parallel implementation of a Monte Carlo PDF algorithm developed for the structured grid calculations on a Cray T3D [6]. The computations were performed in conjunction with a CFD solver and LSPRAY. The parallel algorithm made use of the shared memory constructs exclusive to Cray MPP (Massively Parallel Processing) Fortran and the computations showed a reasonable degree of parallel performance when they were performed on a NASA LeRC Cray T3D with the number of processors ranging between 8 to 32 [6]. Later on, the extension of this method to unstructured grids and parallel computing written in Fortran 77 with PVM or MPI calls was reported in [7-9]. The latest version in Fortran 77/90 offers greater computer platform independence. In this section, we only highlight some important aspects of parallelization from Refs. [6-9].

Both the EUPDF-II and CFD modules are well suited for parallel implementation. For the gas-phase computations, the domain of computation is simply divided into n-Parts of nearly equal size and each part is solved by a different processor. Fig. 2 illustrates a simple example of the domain decomposition strategy adopted for the gas-phase computations where the total domain is simply divided equally amongst the available computer processing elements (PEs). In this case, we assumed the number of available PEs to be equal to four. However, the spray computations are more difficult to parallelize because of its representation based on a Lagrangian formulation. More details on its parallelization can be found in Refs. [6-9].

In the fractional step Monte Carlo method, the steps associated with the spatial transport due to convection and turbulent diffusion as well as the steps associated with the transport in the scalar space due to molecular mixing, spray contribution, and chemical kinetics are advanced in a series of sequential steps

In the parallel implementation of the Monte Carlo PDF code, the inter-processor communications are essentially limited to updating the solution at the interfaces of the inter-processor domain boundaries only once at the beginning of every time step. With the domain decomposition adopted, all the stages of the fractional step Monte Carlo method, associated with such phenomena as the spatial transport associated with convection/diffusion and the transport in the scalar space due to molecular mixing, spray,

Table 2. Description of EUPDF-II Fortran subroutines.

| **Subroutine** | **Purpose of the Subroutines** |
|---|---|
| average(ncyc) | It calculates the ensemble-averaged temperature and species fields based on the averaging scheme selected. |
| coeffiv(axyzp,d) | It calculates the convection/diffusion coefficients as given by $c_n$ and $c_p$ of Eq. 12. |
| convec(axyzp,d) | It performs the task of moving the particles between the neighboring cells during the integration of the convection/ diffusion step as described in Section 6.2. |
| eupdf | This is the main controlling routine for the Monte Carlo PDF solver. When it is called, it updates the PDF solution based on Eq. (5) before returning control over to the calling routine. |
| mimd_pdf (nparti,is,phi1) | It facilitates the inter-processor communications by updating the solution at the interfaces of the inter-processor domain boundaries. |
| mimd_pdf_recv (i_recvfrom, nparti,is, phi1) | It is called by *mimd_pdf* in order to facilitate the inter-processor communications by receiving data from the other processors. |
| mimd_pdf_send (i_sendto, nparti,is,phi1) | It is called by *mimd_pdf* in order to facilitate the inter-processor communications by sending data to the other processors. |
| molmix(freq_dt) | It provides the solution for Eq. (22) - the fractional step associated with the molecular mixing as described in Section 6.4. |
| outpdf1(ncyc) | It calculates the residual errors associated with the PDF solution. |
| outpdf2(ncyc) | It creates the restart files for the next continuation. |
| pdf_chem2 | It provides the solution based on the integration of Eq. (17) - the fractional step associated with the terms arising from the chemical reactions. |
| pdf_int_rerun | It initiates the Monte Carlo PDF computations either by reading the data from the restart files - *ncc_pdf_params.out*, *ncc_pdf_results.db*, and & *ncc_pdf_results_ave.db*, or by initializing the PDF computations to start from the beginning. |
| props_ther | This routine calculates the following properties for use in the CFD solver: (1) temperature, (2) pressure or density depending on the flow being compressible or not , (3) specific heat at constant pressure, and (4) transport properties. |
| ransed(iarg,lu) | It sets up an appropriate seeding for the random number generation. |
| ranu2(x,jdim) | It is a subroutine used in the random number generation. |
| spray | It provides the solution for Eqs. (24)-(25) - the fractional step associated with the spray source terms arising from the exchanges of mass, momentum, and energy with the liquid-phase. |
| vrand(i,x,s,n) | It generates a vector of pseudo-random numbers uniformly distributed on the exclusive interval (0,1) for use on 32 bit machines. |

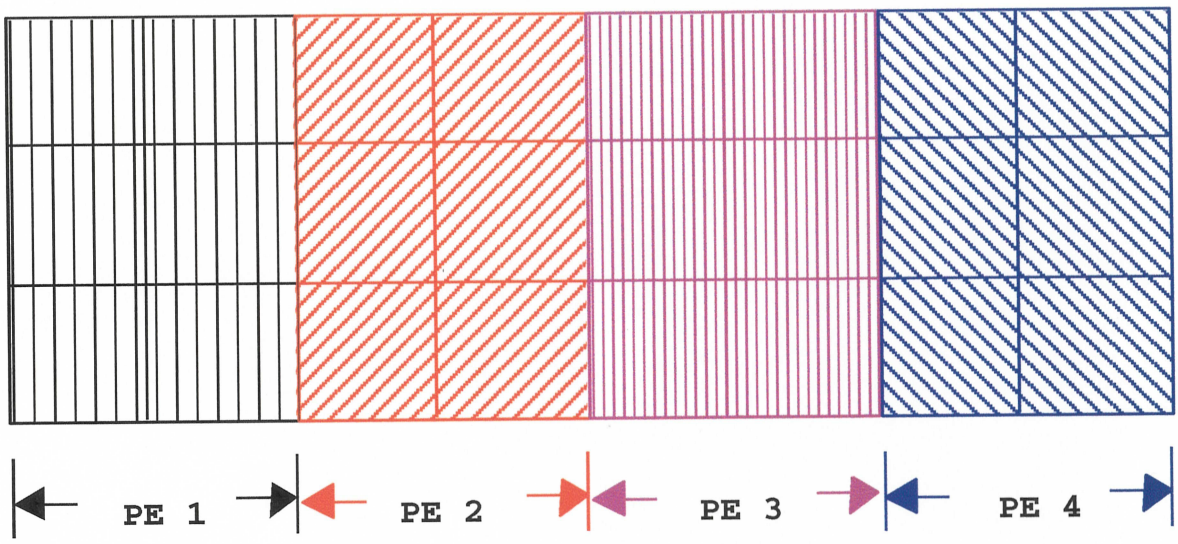


**Fig. 2** An illustration of the parallelization strategy employed in the gas flow computations.

and chemical kinetics, lend themselves perfectly to parallel computing without any need for interprocessor communications during their integration. Therefore, a very high degree of parallelism could easily be achieved if enough care is exercised in distributing the spatial grid points uniformly amongst all the available PEs. Thus, the Monte Carlo simulation is ideally suited for parallel computing and the run time could be considerably minimized by performing the computations on a massively parallel computer.

### 9.1 Details of Parallel Performance

The details of the combined parallel performance of the CFD, EUPDF-II, and LSPRAY codes involving several different cases can be found in Refs. [6-9]. Here, we only summarize briefly the parallel-performance results for two different cases. One is a 3D test case and more details on this case can be found in the reference [8]. For this case, the calculations were performed on a computational grid comprising of 8430 tetrahedral elements and 100 Monte Carlo PDF particles per cell. The computations were performed on one of the NASA Ames Research Center's parallel computer platforms called Turing which is a SGI Origin work-station with 24 PEs (Processor Elements). Table 3 summarizes the CPU times per cycle taken by the EUPDF-II, LSPRAY, and CFD solvers vs the number of PEs. Both the CFD and PDF solvers show good parallel performance with an increase in the number of processors but for the spray solver it shows reasonable parallel performance.

Next, we would like to summarize the results from [9] showing only the results of the PDF and CFD computations. The computations refer to the case of a confined swirl-stabilized spray flame. The computations were performed on LACE (Lewis Advanced Cluster Environment) at NASA LeRC. The computations were performed on a grid with a mesh size of 3600 quadrilateral elements and a total of 0.36 million Monte Carlo particles (=100 particles/cell). Table 4 summarizes the cpu times per cycle taken by the PDF and CFD codes versus the number of processors. Both the PDF and CFD solvers showed good parallel performance with an increase in the number of processors. It takes approximately about 2000 to 5000 cycles for the computations to reach a converged solution.

| Table 3. CPU time (sec) per cycle versus number of PEs. | | | | |
|---|---|---|---|---|
| | | Number of processors | | |
| Solver | Characteristic | 2 | 5 | 10 |
| CFD | 5 steps/cycle | 2.50 | 1.25 | 0.75 |
| EUPDF-II | 1 step/cycle | 6.5 | 2.9 | 1.9 |
| LSPRAY | 100 steps/cycle | 1.70 | 0.64 | 0.53 |

| Table 4. Cpu time (sec) per cycle versus number of PEs on LACE Cluster. | | | | | |
|---|---|---|---|---|---|
| | | Number of processors | | | |
| Solver | Characteristic | 2 | 4 | 8 | 16 |
| EUPDF-II | 1 step/cycle | 2.30 | 1.35 | 0.75 | 0.44 |
| CFD | 5 steps/cycle | 3.55 | 1.90 | 1.10 | 0.60 |

## 10 A SUMMARY OF SOME RECENT VALIDATION CASES

The following eight cases were validated:

1. A supersonic axisymmetric jet involving hydrogen/air combustion.
2. A coaxial supersonic burner involving hydrogen/air combustion.
3. A planar high-subsonic reacting shear layer involving hydrogen/air combustion.
4. A reacting methanol spray with no-swirl.
5. A non-reacting methanol spray with no-swirl.
6. A confined swirl-stabilized n-heptane reacting spray.
7. An unconfined swirl-stabilized n-heptane reacting spray.
8. A confined swirl-stabilized kerosene reacting spray.

The experimental data for the first case was provided by Evans et al [21] and for the second case it was provided by Cheng et al [22]. The validation for Cases 1 and 2 was described by Hsu et al in [4] and [5] and the comparisons showed reasonable agreement. And the experimental data for Case 3 was provided by Chang et al [23] and its validation involving a planar high-subsonic reacting shear layer was reported by Liu & Raju [24].

The experimental data for Cases 4 & 5 was provided by McDonell & Samuelsen from the University of California at Irvine [25]. Both the cases are without swirl; one is a reacting case and the other is non-reacting. The data for Cases 6 & 7 was provided by Bulzan from the NASA Glenn Research Center [26-27]. Both the cases are swirl-stabilized reacting cases, one is an unconfined flame and the other is confined. The data for the last case was provided by El Banhawy & Whitelaw from Imperial College [28]. It is a confined swirl-stabilized kerosene spray flame. Here, we would like to provide a brief summary of the validation cases but a detailed presentation of the results and discussion can be found elsewhere in the papers [6-9]. The comparisons involved both gas and drop velocities, drop size distributions, drop spread-

ing rates, and gas temperatures. The results were in reasonable agreement with the available experimental data. The comparisons also involved the results obtained from the use of the Monte Carlo PDF method as well as those obtained from a conventional CFD solution without the Monte Carlo PDF method. For the case of McDonell & Samuelsen's reacting spray flame, the detailed comparisons clearly highlighted the importance of chemistry/turbulence interactions in the modeling of reacting sprays [8]. The results from the PDF and non-PDF methods were found to be markedly different with the PDF solution providing a better approximation to the reported experimental data. The PDF solution showed that most of the combustion occurred in two distinct flame regions with most of the combustion occurring in a regime that is mostly diffusion controlled and the second regime showing the characteristics of a premixed flame. However, the non-PDF predictions showed incorrectly that most of the combustion occurred in a predominantly vaporization-controlled regime. The Monte Carlo temperature distribution showed that the functional form of the PDF for the temperature fluctuations varied substantially from point to point. The results brought to the fore some of the deficiencies associated with the use of assumed-shape PDF methods in spray computations.

## 11 CONCLUDING REMARKS

- This manual provides a complete description of EUPDF-II - An Eulerian Monte Carlo PDF solver developed for application with parallel computing and unstructured grids.
- We have extended the joint scalar Monte Carlo PDF method to two-phase flows and, thereby, demonstrating the importance of chemistry/turbulence interactions in the modeling of reacting sprays.
- The method outlines several techniques designed to overcome some of the high computer time and storage limitations associated with the Monte Carlo simulation of practical combustor flows.
- It provides the user with a basic understanding of the PDF formulation and the EUPDF-II code structure, and complete details on how to couple the PDF code to other CFD codes.
- The basic structure adopted for the grid representation and parallelization follows the guidelines established for NCC.
- Based on the validation studies involving several spray flames, the results were found to be encouraging in terms of their ability to capture the overall structure of a spray flame.
- The source code of EUPDF-II will be available with NCC as a complete package.

## 12 ACKNOWLEDGEMENT

The research funding for this work was provided by NASA Glenn Research Center with Dr. N.-S. Liu acting as the technical monitor.

## 13 REFERENCES

1. Pope, S.B., "PDF Methods for Turbulent Reactive Flows," Prg. Energy Combust. Sci., Vol. 11, pp. 119-192, 1985.
2. Borghi, R., "Turbulent Combustion Modeling," Prog. Energy Combust. Sci., Vol. 14, pp. 245-292, 1988.
3. Scheurlen, M., Noll, B., and Wittig, S., "Application of Monte Carlo Simulation For Three-Dimensional Flows," In AGARD-CP-510, CFD Techniques For Propulsion Applications, February 1992.
4. A.T. Hsu, Y.-L.P. Tsai, and M.S. Raju, "A Probability Density Function Approach for Compressible Turbulent Reacting Flows," AIAA Journal, Vol. 32, No. 7, pp. 1407-1415, 1994.
5. A.T. Hsu, M.S. Raju, and A.T. Norris, "Application of a pdf Method to Compressible Turbulent Reacting Flows," AIAA 94-0781, AIAA 32nd Aerospace Sciences Meeting, Reno, Nevada, January 1994.
6. M.S. Raju, Application of Scalar Monte Carlo Probability Density Function Method For Turbulent Spray Flames, Numerical Heat Transfer, Part A, vol. 30, pp. 753-777, 1996.
7. M.S. Raju, Current Status of the Use of Parallel Computing in Turbulent Reacting Flows: Computations Involving Sprays, Scalar Monte Carlo Probability Density Function & Unstructured Grids, Advances in Numerical Heat Transfer, vol. 2, ch. 8, pp.259-287, 2000.

8. M.S. Raju, On the Importance of Chemistry/Turbulence Interactions in Spray Computations, Numerical Heat Transfer, Part B: Fundamentals, No. 5, Vol. 41, pp. 409-432, 2002.

9. M.S. Raju, Scalar Monte Carlo PDF Computations of Spray Flames on Unstructured Grids With Parallel Computing, Numerical Heat Transfer, Part B, No. 2, Vol. 35, pp. 185-209, March 1999.

10. M.S. Raju, LSPRAY - A Lagrangian Spray Solver - User's Manual, NASA/CR-97-206240, NASA Lewis Research Center, Cleveland, Ohio, November 1997.

11. M.S. Raju, EUPDF - An Eulerian-Based Monte Carlo Probability Density Function (PDF) Solver - User's Manual, NASA/CR-1998-20401, NASA Lewis Research Center, Cleveland, Ohio, April, 1998.

12. Liu, N.S., and Stubbs, R.M., "Preview of National Combustion Code," AIAA 97-3114, 33rd AIAA/ASME/SAE/ASEE Joint Propulsion Conference, July 6-9, 1997/Seattle, WA.

13. Ryder, R., "CORSAIR User's Manual: Version 1.0," SID: Y965, Pratt and Whitney Engineering, United Technologies Corporation, 25 January 1993.

14. Sirignano, W.A., "Fluid Dynamics of Sprays," Journal of Fluids Engineering, vol. 115, no. 3, pp. 345-378, September 1993.

15. T.-H. Shih, K.-H. Chen, and N.-S. Liu, A Non-Linear $k - \epsilon$ Model for Turbulent Shear Flows, AIAA/ASME/SAE/ASEE 34th Joint Propulsion Conference, Cleveland, Ohio, July 13-15, 1998.

16. Correa, S.M. "Development and Assessment of Turbulence-Chemistry Models in Highly Strained Non-Premixed Flames," AFOSR/NA Contractor Report, 110 Duncan Avenue, Bolling AFB, DC 20332-0001, 31 October, 1994.

17. Anderson, D.A., Tannehill, J.C., and Fletcher, R.H., "Computational Fluid Mechanics and Heat Transfer," Series in Computational Methods in Mechanics and Thermal Sciences, Hemisphere Publishing Corporation, Washington D.C., U.S.A., 1984.

18. Raju, M.S., Liu, W.Q., and Law, C.K., " A Formulation of Combined Forced and Free Convection Past Horizontal and Vertical Surfaces," Int. J. Heat and Mass Transfer, Vol 27, pp. 2215-2224, 1984.

19. Westbrook, C.K. and Dryer, F.L., "Chemical Kinetic Modelling of Hydrocarbon Combustion," Progress in Energy and Combustion Science, Vol. 10, No. 1, 1984, pp. 1-57.

20. Ryan, J.S., and Weeratunga, S.K., "Parallel Computation of 3-D Navier-Stokes Flowfields for Supersonic Vehicles," AIAA 93-0064, 31st Aerospace Sciences Meeting and Exhibit, Reno, NV, 1993.

21. Evans, J.S., Schexnayder, C.J., and Beach, H.L., "Application of a Two-Dimensional Parabolic Computer Program to Prediction of Turbulent Reacting Flows," NASA TP-1169, March 1978.

22. Cheng, T., Wehrmeyer, J.A., Pitz, R.W., Jarrett, O., and Northam, G.B.,"Finite-Rate Chemistry Effects in a Mach 2 Reacting Flow," AIAA 91-2320, Sacramento, CA.

23. Chang, C. T., Marek, C. J., Wey, C., Jones, R. A., and Smith, M. J., "Comparison of Reacting and Non-Reacting Shear Layers at a High Subsonic Mach Number," AIAA-93-2381.

24. Lai, H., and Raju, M.S., "CFD Studies of Subsonic, Turbulent, Planar Shear Layers," The 29th AIAA/SAE/ASME/ASEE Joint Propulsion Conference, Monterey, July 1993.

25. V.G. McDonell and G.S. Samuelson, An Experimental Data Base for the Computational Fluid Dynamics of Reacting and Nonreacting Methanol Sprays, J. Fluids Engineering, vol. 117, pp.145-153, 1995.

26. D.L. Bulzan, Structure of a Swirl-Stabilized, Combusting Spray, NASA Technical Memorandum: NASA TM-106724, Lewis Research Center, Cleveland, Ohio, 1994.

27. D.L. Bulzan, Velocity and Drop Size Measurements in a Confined, Swirl-Stabilized Combusting Spray, AIAA 96-3164, 32rd AIAA/ ASME/ SAE/ ASEE Joint Propulsion Conference, July 01-03, 1996/Buena Vista, FL.

28. Y. El Banhawy and J.H. Whitelaw, Calculation of the Flow Properties of a Confined Kerosene-Spray Flame, AIAA J., vol. 18, no. 12, pp. 1503-1510, 1980

# REPORT DOCUMENTATION PAGE

*Form Approved*
*OMB No. 0704-0188*



| 1. AGENCY USE ONLY (*Leave blank*) | 2. REPORT DATE | 3. REPORT TYPE AND DATES COVERED |
|---|---|---|
| | April 2004 | Final Contractor Report |

**4. TITLE AND SUBTITLE**

EUPDF-II: An Eulerian Joint Scalar Monte Carlo PDF Module
Users' Manual

**5. FUNDING NUMBERS**

WBS–22–714–20–06
NAS3–00145

**6. AUTHOR(S)**

M.S. Raju

**7. PERFORMING ORGANIZATION NAME(S) AND ADDRESS(ES)**

QSS Group, Inc.
21000 Brookpark Road
Cleveland, Ohio 44135

**8. PERFORMING ORGANIZATION REPORT NUMBER**

E–14549

**9. SPONSORING/MONITORING AGENCY NAME(S) AND ADDRESS(ES)**

National Aeronautics and Space Administration
Washington, DC 20546–0001

**10. SPONSORING/MONITORING AGENCY REPORT NUMBER**

NASA CR—2004-213073

**11. SUPPLEMENTARY NOTES**

Project Manager, Dr. Nan-Suey Liu, Turbomachinery and Propulsion Systems Division, NASA Glenn Research Center, organization code 5830, 216–433–8722.

**12a. DISTRIBUTION/AVAILABILITY STATEMENT**

Unclassified - Unlimited
Subject Categories: 02, 08, 07, 01, and 34 Distribution: Nonstandard

Available electronically at http://gltrs.grc.nasa.gov

This publication is available from the NASA Center for AeroSpace Information, 301–621–0390.

**12b. DISTRIBUTION CODE**

**13. ABSTRACT** ***(Maximum 200 words)***

EUPDF–II provides the solution for the species and temperature fields based on an evolution equation for PDF (Probability Density Function) and it is developed mainly for application with sprays, combustion, parallel computing, and unstructured grids. It is designed to be massively parallel and could easily be coupled with any existing gas-phase CFD and spray solvers. The solver accommodates the use of an unstructured mesh with mixed elements of either triangular, quadrilateral, and/or tetrahedral type. The manual provides the user with an understanding of the various models involved in the PDF formulation, its code structure and solution algorithm, and various other issues related to parallelization and its coupling with other solvers. The source code of EUPDF–II will be available with National Combustion Code (NCC) as a complete package.

| 14. SUBJECT TERMS | 15. NUMBER OF PAGES |
|---|---|
| Spray combustion modeling; Sprays: Turbulent reacting flow modeling; CFD; Combustion | 23 |
| | 16. PRICE CODE |

| 17. SECURITY CLASSIFICATION OF REPORT | 18. SECURITY CLASSIFICATION OF THIS PAGE | 19. SECURITY CLASSIFICATION OF ABSTRACT | 20. LIMITATION OF ABSTRACT |
|---|---|---|---|
| Unclassified | Unclassified | Unclassified | |